



## Photon statistics of quantum light on scattering from rotating ground glass

Sheng-Wen Li <sup>1,2</sup>, Fu Li,<sup>2</sup> Tao Peng <sup>2</sup> and G. S. Agarwal <sup>2</sup>

<sup>1</sup>Center for Quantum Technology Research, School of Physics, Beijing Institute of Technology, Beijing 100081, People's Republic of China

<sup>2</sup>Texas A&M University, College Station, Texas 77843, USA



(Received 21 November 2019; revised manuscript received 12 March 2020; accepted 4 May 2020; published 2 June 2020)

When a laser beam passes through a rotating ground glass (RGG), the scattered light exhibits thermal statistics. This is extensively used in speckle imaging. This scattering process has not been addressed in the photon picture and is especially relevant if nonclassical light is scattered by the RGG. We develop the photon picture for the scattering process using the Bose statistics for distributing  $N$  photons in  $M$  pixels. We obtain an analytical form for the  $P$  distribution of the output field in terms of the  $P$  distribution of the input field. In particular, we obtain a general relation for the  $n$ th-order correlation function of the scattered light, i.e.,  $g_{\text{out}}^{(n)} \simeq n! g_{\text{in}}^{(n)}$ , which holds for any order  $n$  and for arbitrary input states. This result immediately recovers the classical transformation of coherent light to pseudothermal light by RGG.

DOI: [10.1103/PhysRevA.101.063806](https://doi.org/10.1103/PhysRevA.101.063806)

### I. INTRODUCTION

Laser light usually carries a (super-)Poisson photon statistics [1–4], but when a laser beam passes through a rotating ground glass (RGG), the scattered light exhibits a thermal statistics.<sup>1</sup> This is known as the “pseudothermal” light, which has been well verified in experiments [5–10], and widely used for ghost imaging [11–13], subwavelength imaging and lithography [14,15], as well as some fundamental studies [16–18].

It is quite interesting that the input Poisson statistics can be changed to be the thermal statistics in such a simple way. Usually this is understood in classical theory [19,20]: the light field  $E$  collected at the photon detector is the superposition of the subfields  $\tilde{E}_i$  propagated from different positions of the RGG. Due to the rotation of the disk, the phases and amplitudes of these subfields  $\tilde{E}_i$  are varying with time randomly. According to the central limit theorem, their summation  $E$ , as a random variable, exhibits a Gaussian distribution [ $P(E) \sim \exp(-\beta|E|^2)$ ], and thus the intensity ( $I \sim |E|^2$ ) exhibits a negative-exponential distribution, i.e., the thermal distribution [19–22].

In principle, the central limit theorem requires the sub-sources  $\tilde{E}_i$  to be infinitely many point sources. Experimentally, the number of sub-sources is limited by the granules within the light spot on the ground glass; thus the pseudothermal light generated in experiments shows some deviation from the ideal thermal distribution [23–25].

Rigorously speaking, the continuous distribution  $P(I)$  for the light intensity is a classical treatment, but not exactly equivalent with the distribution  $P_n$  for the quantized photon

numbers, especially in the few-photon regime. Moreover, if the input light is a nonclassical state, the above classical interpretation does not apply.

In this sense, although the transformation of coherent light on a diffusing glass plate has been extensively investigated [6–10,19,20] and achieved wide applications in speckle imaging [11–13,24–26], most of the time it was based on the above classical understanding rather than a fully quantized photon picture. In particular, if the input light intensity is at single-photon level, or is scattered by very few diffusers, the validity of the above classical theory needs to be checked more carefully.

In this paper, we develop a quantum framework to study the full photon number statistics of such light scattered from general input states. The basic picture is, when  $N_p$  photons are scattered randomly by the RGG, the photon number received by a small area fluctuates stochastically. Therefore, the photon number statistics is obtained by counting the combinations how these photons are randomly distributed on the scattered light pattern, and that naturally gives the thermal statistics.

Further, by taking the input statistics into account, the scattered photon statistics can be well obtained for arbitrary input states, including nonclassical ones. Moreover, we prove that the scattered  $g_{\text{out}}^{(2)}$  is always twice that of the input  $g_{\text{out}}^{(2)} \simeq 2g_{\text{in}}^{(2)}$  for any input states, including nonclassical states. Besides, we also obtain the  $P$  function of the scattered light in the many-diffuser limit, and that further gives the relation  $g_{\text{out}}^{(n)} \simeq n! g_{\text{in}}^{(n)}$  for high-order correlations of any order  $n$  and any input.

The paper is arranged as follows. In Sec. II, we discuss the basic generation mechanism of the pseudothermal light. In Sec. III, we obtain the scattered  $g^{(2)}$  correlation for an arbitrary input state. In Sec. IV, we discuss the scattered  $P$  function and high-order correlations. The summary is drawn in Sec. V.

<sup>1</sup>Throughout this paper, we focus on the “thermal light” with a single frequency, namely, only one optical mode is in the thermal state, and all the other field modes are in the vacuum state.

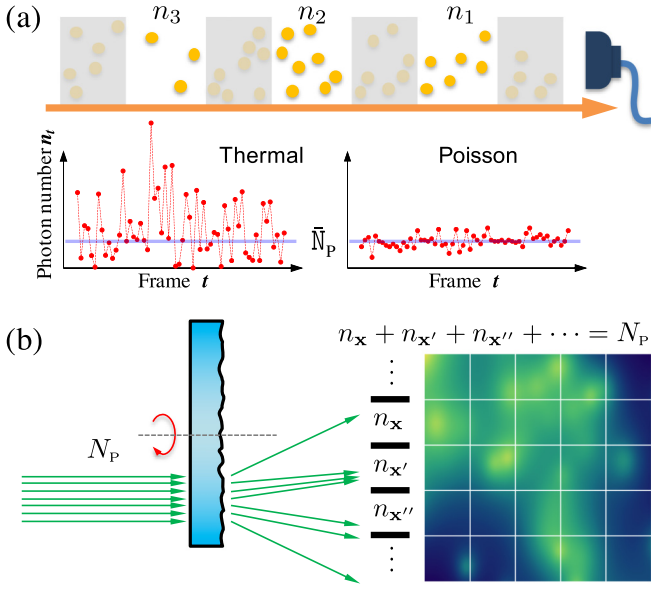


FIG. 1. (a) Demonstration for the photon counting process. (b) The light beam is scattered divergently by the RGG and generates a random light pattern.

## II. THE PSEUDOTHERMAL LIGHT GENERATION FROM PHOTON SCATTERING

We first briefly review the basic photon counting process [Fig. 1(a)]. Considering a steady light flux coming into the photon detector (PD), in each exposure period, a quantum projective measurement is made on the light intensity. The exposure time must be much shorter than the light coherence time, otherwise the measured result is indeed a time average, which corresponds to classical treatments [21,22]. In the idealistic case, the data  $\{n_t\}$  of many exposure frames should be a stochastic series of integers due to the quantized feature of photons, as well as the intrinsic randomness of quantum measurements [27–30]. This can be regarded as multiple repetitive measurements on the same light state. Counting  $\{n_t\}$  gives the photon number distribution  $P_n$  of the incoming light.

Therefore, the pseudothermal light generation can be understood as follows. Considering a laser beam divergently scattered by a RGG, we suppose all the scattered light is collected by a pixel lattice composed of  $M (\gg 1)$  independent PDs. In each exposure, this pixel lattice takes a photo frame of the whole scattered light, which appears as a light pattern randomly distributed in spatial domain [Fig. 1(b)]. When the ground glass is moving, this light pattern varies with time like a “zoetrope” [5,6,24]. Thus, when focusing on a small area on the light pattern, its intensity fluctuates with time stochastically, which is similar to the above quantum measurement data. This is just how the pseudothermal light is obtained.

Thus, the photon statistics on a certain pixel can be calculated by counting how the input photons are distributed on the whole pixel lattice, as shown below.

### A. Fock input

We first consider a simple case that in each frame, the incoming light always contains exactly  $N_p$  photons (Fock input).

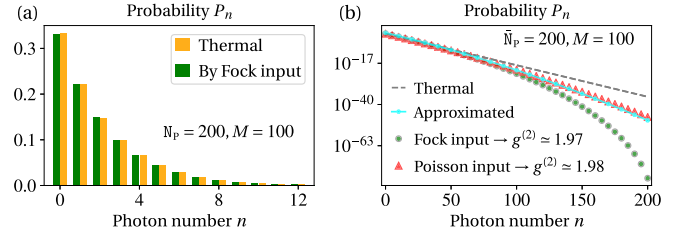


FIG. 2. (a) The scattered photon distribution  $P_n$  on one pixel from Fock input (left green), comparing with the thermal one (right yellow) with the same mean photon number. (b) The scattered photon distribution (in logarithmic scale) from the Fock and Poisson input ( $\bar{N}_p = 200$ ) comparing with the thermal distribution (dashed gray line). The dotted cyan line is the approximated result (7).

Due to the stochastic scattering, these  $N_p$  photons would be randomly distributed to all the  $M$  pixels. Denoting  $n_{\mathbf{x},t}$  as the photon number recorded at pixel  $\mathbf{x}$  in frame  $t$ , all possible pattern configurations  $\{n_{\mathbf{x}}\}$  may appear (assuming with equal probabilities). Remember all  $n_{\mathbf{x}}$  are integers ( $0 \leq n_{\mathbf{x}} \leq N_p$ ), and they must satisfy the constraint of energy conservation  $\sum_{\mathbf{x}} n_{\mathbf{x}} = N_p$ . Thus, since photons are identical bosons, the total number of such combinations is given by [see Eq. (55.4) in Ref. [31]]<sup>2</sup>

$$Z := \binom{N_p + M - 1}{M - 1} = \frac{(N_p + M - 1)!}{(M - 1)! N_p!}. \quad (1)$$

Further, we count the probability that  $n$  photons are received by a single pixel. That is equivalent to counting the combinations of how  $N_p - n$  photons are distributed on the rest of the  $M - 1$  pixels, which gives (for  $M \geq 2$ )

$$P_n^{(N_p)} = \begin{cases} \frac{1}{Z} \binom{N_p - n + M - 2}{M - 2}, & 0 \leq n \leq N_p \\ 0, & n > N_p. \end{cases} \quad (2)$$

This is just the scattered photon statistics on one pixel when the input light carries  $N_p$  photons in each frame.

In the regime  $n \ll N_p$ , the above probability gives

$$\frac{P_{n+1}^{(N_p)}}{P_n^{(N_p)}} = \frac{1}{1 + \frac{M-2}{N_p-n}} \simeq \frac{1}{1 + M/N_p}, \quad (3)$$

which is a constant and less than 1 (when  $M \gg 1$ ). That means, the statistics received on this pixel well exhibits the thermal distribution. In the regime  $n \sim N_p$ , the deviation from the ideal thermal distribution gradually grows larger, but this difference is not easy to observe in practical experiments (Fig. 2).

Therefore, when focusing on the photon statistics received on a local area, the conservation constraint of the total photon number naturally leads to the thermal statistics. Indeed this is quite similar to the mechanism for how the canonical ensemble with the thermal statistics emerges as a subsystem inside a bigger microcanonical one in statistical physics [31,32].

<sup>2</sup>This is equivalent to counting the combinations of how  $N_p$  identical balls are put into  $M$  different boxes, with zero reception allowed.

### B. Poisson input

The incoming light could also have certain distribution  $\mathcal{P}_{\text{in}}(N)$  but not exactly  $N_{\text{p}}$  photons. In this case, taking the input statistics into account, the scattered statistics is

$$P_n = \sum_N \mathcal{P}_{\text{in}}(N) P_n^{(N)}, \quad (4)$$

where  $P_n^{(N)}$  is the result from the scattering of  $N$  photons [Eq. (2)].

For a laser input, the input statistics  $\mathcal{P}_{\text{in}}(N)$  is approximately a Poisson distribution, which is narrowly distributed around its mean value  $\bar{N}_{\text{p}}$  with a relatively small variance ( $\sqrt{\langle \delta n^2 \rangle} / \langle n \rangle = 1 / \sqrt{\bar{N}_{\text{p}}}$ ). Therefore, in the above summation (4), only the terms around  $N \simeq \bar{N}_{\text{p}}$  contribute significantly. As a result, approximately the output photon statistics is also a thermal one, which satisfies

$$\frac{P_{n+1}}{P_n} \simeq \frac{1}{1 + M/\bar{N}_{\text{p}}}. \quad (5)$$

For the above Fock and Poisson input cases, the exact output distributions  $P_n$  are numerically shown in Figs. 2(a) and 2(b), and they are both quite close to the thermal distribution in the regime  $n \ll \bar{N}_{\text{p}}$ . When the photon number  $n$  is large, both of them deviate from the thermal one.

Generally, the input light state may also contain quantum coherences between the Fock states (e.g., the coherent state  $|\alpha\rangle = \sum_n e^{-|\alpha|^2/2} / \sqrt{n!} |n\rangle$ ), or between the different scattered spatial modes. But the RGG randomizes phases, thus the measurement on the photon number  $\hat{N}$  is directly related to the photon number distribution  $P_n$  and the off-diagonal elements do not take effect (see p. 127 in Ref. [33]).

### C. Nonthermal correction

Here we give an approximated distribution taking into account the above nonthermal correction. We expand the above iterative relation (3) as follows:

$$\begin{aligned} \ln P_{n+1}^{(N_{\text{p}})} - \ln P_n^{(N_{\text{p}})} &= \ln \frac{1}{1 + \frac{M-2}{N_{\text{p}}-n}} \\ &\simeq \ln \frac{1}{1 + \frac{M-2}{N_{\text{p}}}} - n \frac{M-2}{N_{\text{p}}(N_{\text{p}} + M - 2)} + o(n^2). \end{aligned} \quad (6)$$

Omitting the high-order terms  $o(n^2)$ , the summation over  $n$  on both sides gives the following approximated distribution [the dotted cyan line in Fig. 2(b)]:

$$\begin{aligned} P_n^{(N_{\text{p}})} &= P_0 e^{-\beta_0 n - \beta_c (n^2 - n)}, \\ \beta_0 &= \ln \left( 1 + \frac{M-2}{N_{\text{p}}} \right), \quad \beta_c = \frac{1}{2} \frac{M-2}{N_{\text{p}}(N_{\text{p}} + M - 2)}, \end{aligned} \quad (7)$$

where  $P_0$  is a normalization constant. A quadratic correction appears in the exponential factor, and the correction  $\beta_c$  is negligible for strong input  $N_{\text{p}}$ . Indeed, this is a typical non-canonical feature resulted from finite system sizes or coupling strengths [34,35].

Lastly we remark that the ‘‘pixels’’ in the above discussions do not correspond to realistic detector pixels directly. The

sizes of such pixels are determined by the spatial correlation length of the scattered light pattern, so they can be regarded as independent fluctuation units. And their total number  $M$  is roughly determined by the granules within the light spot on the RGG, which is usually a very large number in practice.

### III. THE SCATTERED STATISTICS FROM NONCLASSICAL LIGHT

Without loss of generality, here we have assumed the input photons have a uniform spatial distribution as done in the classical theory. Since usually the imaging area is much larger than coherence length, this is expected to hold well, and the nonuniformity at the edges is not significant.

Generally, the quantum light state can be written in the Glauber-Sudarshan  $P$  representation  $\hat{\rho} = \int d^2\alpha P(\alpha) |\alpha\rangle\langle\alpha|$ , and it has a form of a probabilistic ensemble of coherent states  $|\alpha\rangle$ , which corresponds to classical planar waves. But here the  $P$  function  $P(\alpha)$  may not be positive definite (e.g., the Fock state, sub-Poissonian state), and thus cannot be regarded as the probability distribution. Therefore, in quantum optics, (non-)classical states refer to those who (do not) have a positive  $P(\alpha)$  [4,36].

Thus, for a nonclassical input state, the above standard classical theory based on the central limit theorem does not apply [19,20]. In this case, the scattered photon statistics  $P_n$  still can be obtained from our Eq. (4).

But the photon number distribution  $P_n$  and the  $P$  function are not easily measured directly. In experiments, it is the  $n$ th-order correlation function of the light state that is more often measured, i.e.,

$$g^{(n)} := \frac{\langle (\hat{a}^\dagger)^n \hat{a}^n \rangle}{\langle \hat{a}^\dagger \hat{a} \rangle^n} = \frac{\sum_m P_m \frac{m!}{(m-n)!}}{\left( \sum_m m P_m \right)^n}, \quad (8)$$

which is a more precise indicator to test the nonclassicality of the light state [4,36]. Considering averagely  $\bar{N}_{\text{p}} = 8$  photons scattered onto  $M = 8$  fluctuating units, although the scattered  $P_n$  from both Fock and Poisson inputs look quite close to the thermal one [Fig. 3(a)], indeed their second-order correlations are  $g_{\text{out}}^{(2)} \simeq 1.556$  (Fock input) and  $g_{\text{out}}^{(2)} \simeq 1.778$  (Poisson input), which both deviate significantly from the thermal result  $g_{\text{th}}^{(2)} = 2$ . When  $g^{(2)} < 1$ , the light state is a nonclassical one [4,36].

For arbitrary input states, the scattered  $g^{(2)}$  correlation can be calculated from Eq. (4). The mean photon number of the scattered light is  $\langle n \rangle = \langle N \rangle_{\text{in}} / M$ , and the mean square is

$$\begin{aligned} \langle n^2 \rangle &= \sum_{N,n} \mathcal{P}_{\text{in}}(N) n^2 P_n^{(N)} = \sum_N \mathcal{P}_{\text{in}}(N) \frac{N(2N + M - 1)}{M(M + 1)} \\ &= \frac{2\langle N^2 \rangle_{\text{in}}}{M(M + 1)} + \frac{\langle N \rangle_{\text{in}}(M - 1)}{M(M + 1)}. \end{aligned} \quad (9)$$

Then after simple calculations, the scattered  $g_{\text{out}}^{(2)} = (\langle n^2 \rangle - \langle n \rangle^2) / \langle n \rangle^2$  can be represented by the input  $g_{\text{in}}^{(2)}$ :

$$g_{\text{out}}^{(2)} = \frac{2(\langle N^2 \rangle_{\text{in}} - \langle N \rangle_{\text{in}}^2) M}{\langle N \rangle_{\text{in}}^2 (M + 1)} = 2g_{\text{in}}^{(2)} \frac{M}{M + 1}. \quad (10)$$

In practice, the RGG usually has a large number of diffusers ( $M \gg 1$ ), which gives  $g_{\text{out}}^{(2)} \simeq 2g_{\text{in}}^{(2)}$ . It is worth noting

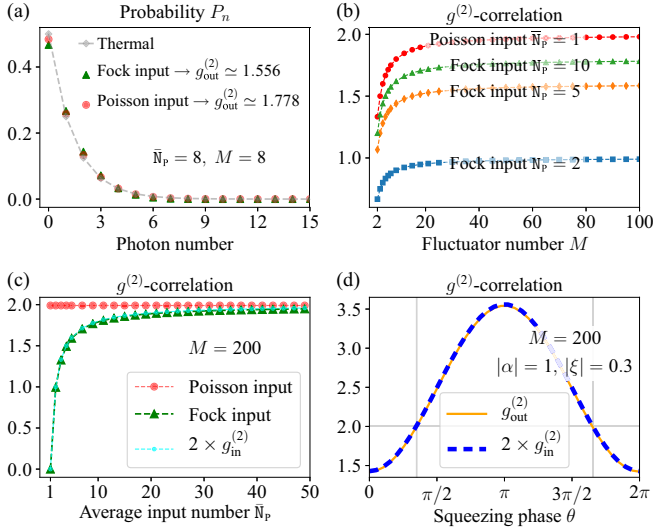


FIG. 3. (a) The scattered distribution  $P_n$  from Fock and Poisson input ( $\bar{N}_p = 8, M = 8$ ). (b) The scattered  $g_{out}^{(2)}$  from Fock ( $N_p = 2, 5, 10$ ) and Poisson input ( $\bar{N}_p = 1$ ) changing with fluctuator number  $M$ . (c) The scattered  $g_{out}^{(2)}$  changing with the input photon number (given  $M = 200$ ), comparing with the input  $g_{in}^{(2)}$  of the Fock state. (d) The scattered  $g_{out}^{(2)}$  from squeezed input changing with the squeezing phase  $\theta$ , comparing with the input  $g_{in}^{(2)}$ .

that this is a general result for arbitrary input statistics, including nonclassical light.

Therefore, a laser input with Poisson statistics always leads to the thermal result  $g_{out}^{(2)} \simeq 2$ , irregardless of the input intensity, even at the single-photon level  $\bar{N}_p = 1$ .

To the contrary, the Fock input  $|N_p\rangle$  has  $g_{in}^{(2)} = 1 - N_p^{-1} \in [0, 1)$ , and that makes the scattered  $g_{out}^{(2)} \simeq 2g_{in}^{(2)}$  increase with the input photon number  $N_p$  [Fig. 3(c)]. In particular, the single-photon input ( $N_p = 1$ ) leads to a scattered state  $\hat{\rho}_{out} = (1 - \frac{1}{M})|0\rangle\langle 0| + \frac{1}{M}|1\rangle\langle 1|$  [by Eq. (2)] which gives  $g_{out}^{(2)} = 0$ .

Thus, the quantum features of nonclassical states appear more significant in the few-photon regime. And it is also worth noting that the Poisson input plays a part in better producing the thermal statistics than the Fock input, since it always guarantees  $g_{out}^{(2)} \simeq 2$ , irregardless of the input intensity.

With the increase of the total number  $M$  of the fluctuating units, the scattered  $g_{out}^{(2)}$  increases and converges to  $g_{out}^{(2)} \simeq 2g_{in}^{(2)}$  [Fig. 3(b)]. And this just corresponds to the condition of infinite diffusers required by the central limit theorem in classical theory.

By utilizing the squeezed light, a nonclassical input state with sub-Poisson statistics can be realized in experiments [4,36,37]. In Fig. 3(d) we show the scattered  $g_{out}^{(2)}$  from the squeezed light calculated from Eq. (4). The input statistics  $\mathcal{P}_{in}(N)$  comes from the squeezed state  $|\alpha, \xi\rangle = \hat{D}_\alpha \hat{S}_\xi |0\rangle$ , where  $\hat{S}_\xi := \exp[\frac{1}{2}(\xi^* \hat{a}^2 - \xi \hat{a}^{\dagger 2})]$ ,  $\hat{D}_\alpha := \exp[\alpha \hat{a}^\dagger - \alpha^* \hat{a}]$  are the squeezing and displacement operators, with  $\xi = re^{i\theta}$  ( $r \geq 0$ ) as the squeezing parameter [4,36].

For different squeezing phases  $\theta$ , the mean photon number remains  $\bar{N}_p = |\alpha|^2 + \sinh^2 r$ , while the input statistics gives sub-Poisson ( $g_{in}^{(2)} < 1$ ) or super-Poisson ( $g_{in}^{(2)} > 1$ ) distribu-

tions. In the whole regime the above relation  $g_{out}^{(2)} \simeq 2g_{in}^{(2)}$  well applies.

Notice that the output light can be used as the input light for further scattering through another RGG; then that gives  $g_{out-2}^{(2)} \simeq 2g_{out-1}^{(2)} \simeq 2^2 g_{in}^{(2)}$ . Clearly, after the hierarchy scattering through  $k$  RGGs, the final output light has  $g_{out-k}^{(2)} \simeq 2^k g_{in}^{(2)}$ . In particular, if the original input is laser, the final output gives  $g_{out-k}^{(2)} \simeq 2^k$  [19,20,38].

In addition, similarly to Eq. (9), the third-order expectation  $\langle n^3 \rangle$  and  $g_{out}^{(3)}$  also can be obtained, i.e.,

$$\langle n^3 \rangle = \frac{6\langle N^3 \rangle_{in} + 6(M-1)\langle N^2 \rangle_{in} + (M^2 - 3M + 2)\langle N \rangle_{in}}{M(M+1)(M+2)},$$

$$g_{out}^{(3)} = \frac{\langle \hat{a}^{\dagger 3} \hat{a}^3 \rangle_{out}}{\langle \hat{a}^\dagger \hat{a} \rangle_{out}^3} = 6g_{in}^{(3)} \frac{M^2}{M^2 + 3M + 2}, \quad (11)$$

which gives  $g_{out}^{(3)} \simeq 6g_{in}^{(3)}$  for large  $M$ . But the calculation of higher orders becomes more and more troublesome. In the following, with the help of the  $P$  function of the scattered light, we can prove  $g_{out}^{(n)} \simeq n! g_{in}^{(n)}$  for any order  $n$  and any input state.

#### IV. THE $P$ FUNCTION OF THE SCATTERED LIGHT AND THE HIGH-ORDER CORRELATIONS

The nonclassical properties of a light state can be more clearly characterized by its  $P$  function [3,4,39], and here we show the  $P$  function of the scattered light and its high-order correlations. As seen above, the Poisson input plays a part in better producing the thermal statistics than the Fock input, since it always leads to the thermal result  $g_{out}^{(2)} \simeq 2$  in spite of the input intensity (in the many-diffuser limit  $M \rightarrow \infty$ ). Thus, approximately this can be written as the following mapping relation:

$$\hat{\rho}_{in} = |\alpha_0\rangle\langle \alpha_0| \rightarrow \hat{\rho}_{out} = \sum \frac{\bar{N}_T^m}{(1 + \bar{N}_T)^{m+1}} |n\rangle\langle n|,$$

$$P_{in}(\alpha) = \delta^{(2)}(\alpha - \alpha_0) \rightarrow P_{out}(\alpha) = \frac{1}{\pi \bar{N}_T} \exp\left(-\frac{|\alpha|^2}{\bar{N}_T}\right). \quad (12)$$

Here  $|\alpha_0|^2$  and  $\bar{N}_T = |\alpha_0|^2/M$  are the mean photon numbers of the input and output statistics. The coherent state  $|\alpha_0\rangle$  always gives the same output with the above probabilistic Poisson input, since the quantum coherences do not take part in the photon counting.

This input-output relation can be written as a linear functional transformation  $P_{out}(\alpha) = \mathcal{F}_\alpha[P_{in}(\alpha)]$ . Then for a general input state  $P_{in}(\alpha) = \int d^2\zeta P_{in}(\zeta) \delta^{(2)}(\alpha - \zeta)$ , the output  $P$  function is

$$P_{out}(\alpha) = \mathcal{F}_\alpha[P_{in}(\alpha)] = \int d^2\zeta P_{in}(\zeta) \mathcal{F}_\alpha[\delta^{(2)}(\alpha - \zeta)]$$

$$= \int d^2\zeta P_{in}(\zeta) \frac{1}{\pi |\zeta|^2/M} \exp\left(-\frac{|\alpha|^2}{|\zeta|^2/M}\right). \quad (13)$$

First, we use Eq. (13) to obtain the high-order moments of

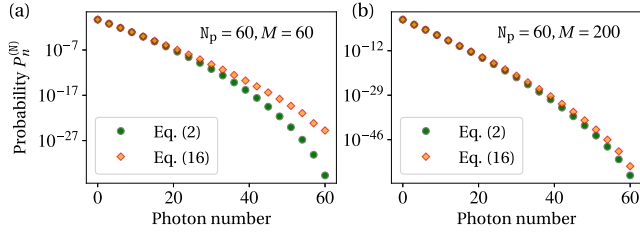


FIG. 4. The scattered distribution  $P_n$  from Fock input ( $N_p = 60$ ) calculated from Eq. (2) (based on combination counting) and Eq. (17) [based on the mapping relation (12)] for (a)  $M = 60$  and (b)  $M = 200$ . For large  $M$ , they almost coincide with each other.

the scattered light,

$$\begin{aligned} \langle \hat{a}^{\dagger n} \hat{a}^n \rangle_{\text{out}} &= \int d^2\alpha |\alpha|^{2n} P_{\text{out}}(\alpha) \\ &= \int d^2\zeta \int d^2\alpha \frac{M}{\pi|\zeta|^2} e^{-(M/|\zeta|^2)|\alpha|^2} |\alpha|^{2n} P_{\text{in}}(\zeta) \\ &= \int d^2\zeta P_{\text{in}}(\zeta) \frac{|\zeta|^{2n}}{M^n} n! = \langle \hat{a}^{\dagger n} \hat{a}^n \rangle_{\text{in}} \cdot \frac{n!}{M^n}. \end{aligned} \quad (14)$$

Therefore, for arbitrary input states, the  $n$ th-order correlation function of the scattered light is

$$g_{\text{out}}^{(n)} = \frac{\langle \hat{a}^{\dagger n} \hat{a}^n \rangle_{\text{out}}}{(\langle \hat{a}^{\dagger} \hat{a} \rangle_{\text{out}})^n} = \frac{n! \langle \hat{a}^{\dagger n} \hat{a}^n \rangle_{\text{in}} / M^n}{(\langle \hat{a}^{\dagger} \hat{a} \rangle_{\text{in}} / M)^n} = n! g_{\text{in}}^{(n)}. \quad (15)$$

This result holds for arbitrary input statistics. In particular, the second order gives  $g_{\text{out}}^{(2)} = 2g_{\text{in}}^{(2)}$ , which is just the result (10) in the many-diffuser limit  $M \rightarrow \infty$ . After the hierarchy scattering through  $k$  RGGs, the final output light gives  $g_{\text{out-k}}^{(n)} \simeq (n!)^k g_{\text{in}}^{(n)}$ .

Next we use the output  $P$  function (13) to obtain the photon statistics, and compare it with the above result (2) based on combination counting. Since the scattered state can be written as  $\hat{\rho}_{\text{out}} = \int d^2\alpha P_{\text{out}}(\alpha) |\alpha\rangle\langle\alpha| = \sum \tilde{P}_n |n\rangle\langle n|$ , the photon number distribution  $\tilde{P}_n$  also can be obtained as

$$\begin{aligned} \tilde{P}_n &= \langle n | \hat{\rho}_{\text{out}} | n \rangle = \int d^2\alpha P_{\text{out}}(\alpha) \frac{|\alpha|^{2n}}{n!} e^{-|\alpha|^2} \\ &= \int d^2\zeta P_{\text{in}}(\zeta) \frac{M/|\zeta|^2}{(1 + M/|\zeta|^2)^{n+1}}. \end{aligned} \quad (16)$$

For a Fock input state  $|N\rangle$ , the input  $P$  function is  $P_{\text{in}}(\zeta) = e^{|\zeta|^2} [\partial_{\zeta}^N \partial_{\zeta^*}^N \delta^{(2)}(\zeta)] / N!$  [4], and the above integral gives

$$\tilde{P}_n^{(N)} = \lim_{\zeta \rightarrow 0} \frac{1}{N!} \partial_{\zeta}^N \partial_{\zeta^*}^N \left[ \frac{e^{|\zeta|^2} M/|\zeta|^2}{(1 + M/|\zeta|^2)^{n+1}} \right]$$

$$= \frac{N!}{n!} \sum_{k=n}^N \frac{(-1)^{k-n} k!}{(N-k)! (k-n)! M^k}, \quad (17)$$

and  $\tilde{P}_n^{(N)} = 0$  for  $n > N$  (see Appendix).

Here we emphasize that Eqs. (16) and (17) are valid only in the many-diffuser limit  $M \rightarrow \infty$ , which guarantees the Poisson input must exactly produce the thermal state and  $g_{\text{out}}^{(2)} = 2g_{\text{in}}^{(2)}$  holds exactly. Thus, generally  $\tilde{P}_n^{(N)}$  is not equivalent with the result (2) based on combination counting, which applies in more general cases. When  $M$  is large, their difference becomes negligible, especially in the few-photon regime (Fig. 4).

## V. SUMMARY

In this paper, we develop a quantum framework to study the full photon number statistics of the scattered light passing through the RGG. The output statistics is obtained by counting the combinations of how the input photons are distributed on the scattered light pattern. When the total photon number of the whole scattered light pattern is approximately a constant, counting the photon number received by a small area on the light pattern naturally gives the thermal statistics. Then for arbitrary input states, the scattered photon statistics also can be well obtained by taking the input statistics into account.

We also obtain the  $P$  function of the scattered light from arbitrary input states in the many-diffuser limit. With the help of these distributions, we find that the scattered light always gives a general relation  $g_{\text{out}}^{(n)} \simeq n! g_{\text{in}}^{(n)}$ , which holds for any order  $n$  and any input state, including nonclassical ones. In these situations, this theory provides a more precise description beyond the previous classical theory based on the central limit theorem.

The above results of  $g^{(n)}$  correlations scattered from nonclassical input can be verified by squeezed light in current experiments, and may be utilized for correlation imaging of high orders. This result also indicates it is possible to create a scattered light with very high  $g^{(n)}$  correlations simply, which may be utilized to enhance the multiphoton absorption processes and high harmonic generation [40–42].

## ACKNOWLEDGMENTS

S.-W. Li appreciates the helpful discussion with R. Nessler, W.-K. Yu, and J. Sperling. This study is supported by NSF of China (Grant No. 11905007), Beijing Institute of Technology Research Fund Program for Young Scholars, AFOSR Award FA-9550-18-1-0141, ONR Award N00014-16-1-3054, and Robert A. Welch Foundation Award A-1261 and A-1943-20180324.

## APPENDIX: CALCULATION OF EQ. (17)

The  $P$  function of the Fock state  $|N\rangle$  is a highly singular function  $P_{\text{in}}(\zeta) = e^{|\zeta|^2} [\partial_{\zeta}^N \partial_{\zeta^*}^N \delta^{(2)}(\zeta)] / N!$ , which contains the derivative of the  $\delta$  function. Notice that for  $\zeta = \zeta_x + i\zeta_y$ , the derivative gives  $\partial_{\zeta} \partial_{\zeta^*} = \frac{1}{4}(\partial_{\zeta_x}^2 + \partial_{\zeta_y}^2) = \frac{1}{4}\nabla^2$ . From the Stokes

theorem we obtain  $\int d^2\zeta [f(\zeta)\nabla^{2n}\delta^{(2)}(\zeta) - \delta^{(2)}(\zeta)\nabla^{2n}f(\zeta)] = 0$ , thus the integral (16) gives

$$\begin{aligned}\tilde{P}_n &= \frac{1}{N!} \int d^2\zeta \left[ \frac{\partial^{2N}}{\partial \zeta^N \partial \zeta^{*N}} \delta^{(2)}(\zeta) \right] e^{|\zeta|^2} \frac{M/|\zeta|^2}{(1+M/|\zeta|^2)^{n+1}} = \frac{1}{N!} \int d^2\zeta \delta^{(2)}(\zeta) \frac{\partial^{2N}}{\partial \zeta^N \partial \zeta^{*N}} \frac{e^{|\zeta|^2} M/|\zeta|^2}{(1+M/|\zeta|^2)^{n+1}} \\ &= \lim_{\zeta \rightarrow 0} \frac{1}{N!} \partial_{\zeta}^N \partial_{\zeta^*}^N \left[ \frac{e^{|\zeta|^2} M/|\zeta|^2}{(1+M/|\zeta|^2)^{n+1}} \right].\end{aligned}\quad (\text{A1})$$

Now we need to calculate this derivative and take the limit. Denoting  $\zeta \rightarrow x$ ,  $\zeta^* \rightarrow y$ , the above derivative gives

$$\begin{aligned}\partial_y^N \left[ \frac{e^{xy} M(xy)^n}{(M+xy)^{n+1}} \right] &= \sum_{k=0}^N C_N^k \partial_y^{N-k} e^{xy} \partial_y^k \frac{M(xy)^n}{(M+xy)^{n+1}} = \sum_{k=0}^N C_N^k e^{xy} x^{N-k} \sum_{q=0}^k C_k^q \partial_y^q [M(xy)^n] \partial_y^{k-q} \frac{1}{[M+xy]^{n+1}} \\ &= \sum_{k=0}^N \sum_{q=0}^k C_N^k C_k^q e^{xy} x^{N-k} M x^n \frac{n!}{(n-q)!} y^{n-q} (-1)^{k-q} \frac{(n+k-q)!}{n!} (M+xy)^{-n-1-k+q} x^{k-q} \\ &= M \sum_{k=0}^N \sum_{q=0}^k \frac{(-1)^{k-q} (n+k-q)!}{(n-q)!} C_N^k C_k^q [y^{n-q} x^{N-q+n} e^{xy} (M+xy)^{-n-1-k+q}].\end{aligned}\quad (\text{A2})$$

Now we need to further calculate the derivative  $\partial_x^N$  by applying the Leibniz rule to the above bracket, which gives  $\sum_{l=0}^N C_N^l [\partial_x^l x^{N-q+n}] \partial_x^{N-l} [e^{xy} (M+xy)^{-n-1-k+q}]$ .

Since lastly we need to take the limit  $x, y \rightarrow 0$ , from the power factor  $\partial_x^l x^{N-q+n} = \frac{(N-q+n)!}{(N-q+n-l)!} x^{N-q+n-l}$  we can notice that only a few terms in the above summations could exist, and they must satisfy  $N-q+n-l=0$ , thus we have  $q-n=N-l \geq 0$ . But since the denominator of Eq. (A2) contains  $(n-q)!$  which gives  $+\infty$  for  $n < q$ , that guarantees  $q=n$  and  $l=N$ . Therefore, taking the limit of the above derivative gives

$$\lim_{x,y \rightarrow 0} \partial_x^N \partial_y^N \left[ \frac{e^{xy} M(xy)^n}{(M+xy)^{n+1}} \right] = \sum_{k=0}^N (-1)^{k-n} k! \frac{N!}{(N-k)! k!} \frac{k!}{(k-n)! n!} \frac{N!}{M^k},\quad (\text{A3})$$

as shown in the main text.

- 
- [1] M. Scully and W. E. Lamb, *Phys. Rev. Lett.* **16**, 853 (1966).  
[2] M. O. Scully and W. E. Lamb, *Phys. Rev.* **159**, 208 (1967).  
[3] M. O. Scully and M. S. Zubairy, *Quantum Optics* (Cambridge University press, Cambridge, UK, 1997).  
[4] G. S. Agarwal, *Quantum Optics*, 1st ed. (Cambridge University Press, Cambridge, UK, 2012).  
[5] W. Martienssen and E. Spiller, *Am. J. Phys.* **32**, 919 (1964).  
[6] F. T. Arecchi, *Phys. Rev. Lett.* **15**, 912 (1965).  
[7] F. Arecchi, A. Berne, A. Sona, and P. Burlamacchi, *IEEE J. Quantum Electron.* **2**, 341 (1966).  
[8] F. T. Arecchi, A. Berné, and P. Bulamacchi, *Phys. Rev. Lett.* **16**, 32 (1966).  
[9] L. E. Estes, L. M. Narducci, and R. A. Tuft, *J. Opt. Soc. Am.* **61**, 1301 (1971).  
[10] P. R. Pearl and G. J. Troup, *Opto-electronics* **1**, 152 (1969).  
[11] A. Gatti, E. Brambilla, M. Bache, and L. A. Lugiato, *Phys. Rev. Lett.* **93**, 093602 (2004).  
[12] A. Valencia, G. Scarcelli, M. D'Angelo, and Y. Shih, *Phys. Rev. Lett.* **94**, 063601 (2005).  
[13] F. Ferri, D. Magatti, A. Gatti, M. Bache, E. Brambilla, and L. A. Lugiato, *Phys. Rev. Lett.* **94**, 183602 (2005).  
[14] D.-Z. Cao, G.-J. Ge, and K. Wang, *Appl. Phys. Lett.* **97**, 051105 (2010).  
[15] F. Li, C. Altuzarra, T. Li, M. O. Scully, and G. S. Agarwal, *J. Opt.* **21**, 115604 (2019).  
[16] T. Peng, H. Chen, Y. Shih, and M. O. Scully, *Phys. Rev. Lett.* **112**, 180401 (2014).  
[17] T. Peng, J. Simon, H. Chen, R. French, and Y. Shih, *Europhys. Lett.* **109**, 14003 (2015).  
[18] Y. S. Ihn, Y. Kim, V. Tamma, and Y.-H. Kim, *Phys. Rev. Lett.* **119**, 263603 (2017).  
[19] J. W. Goodman, *Statistical Optics*, 1st ed. (Wiley-Interscience, New York, 2000).  
[20] J. W. Goodman, *Speckle Phenomena in Optics*, 1st ed. (W. H. Freeman, Englewood, CO, 2010).  
[21] L. Mandel, *Proc. Phys. Soc.* **72**, 1037 (1958).  
[22] L. Mandel, *Proc. Phys. Soc.* **74**, 233 (1959).  
[23] T. Mehringer, S. Mährlein, J. von Zanthier, and G. S. Agarwal, *Opt. Lett.* **43**, 2304 (2018).  
[24] N. Bender, H. Yılmaz, Y. Bromberg, and H. Cao, *Optica* **5**, 595 (2018).  
[25] N. Bender, H. Yılmaz, Y. Bromberg, and H. Cao, *Opt. Express* **27**, 6057 (2019).  
[26] J. H. Shapiro and R. W. Boyd, *Quantum Inf. Process.* **11**, 949 (2012).  
[27] J. Sperling, W. Vogel, and G. S. Agarwal, *Phys. Rev. Lett.* **109**, 093601 (2012).

- [28] J. Sperling, W. Vogel, and G. S. Agarwal, *Phys. Rev. A* **85**, 023820 (2012).
- [29] L. A. Jiang, E. A. Dauler, and J. T. Chang, *Phys. Rev. A* **75**, 062325 (2007).
- [30] B. E. Kardynał, Z. L. Yuan, and A. J. Shields, *Nat. Photonics* **2**, 425 (2008).
- [31] L. Landau and E. Lifshitz, *Statistical Physics, Part 1* (Butterworth-Heinemann, Oxford, 1980).
- [32] K. Huang, *Statistical Mechanics*, 2nd ed. (Wiley, New York, 1987).
- [33] L. Mandel and E. Wolf, *Optical Coherence and Quantum Optics*, 1st ed. (Cambridge University Press, Cambridge, UK, 1995).
- [34] D. Z. Xu, S.-W. Li, X. F. Liu, and C. P. Sun, *Phys. Rev. E* **90**, 062125 (2014).
- [35] H. Dong, S. Yang, X. F. Liu, and C. P. Sun, *Phys. Rev. A* **76**, 044104 (2007).
- [36] C. C. Gerry and P. Knight, *Introductory Quantum Optics* (Cambridge University Press, Cambridge, UK, 2005).
- [37] R. Liu, A. Fang, Y. Zhou, P. Zhang, S. Gao, H. Li, H. Gao, and F. Li, *Phys. Rev. A* **93**, 013822 (2016).
- [38] Y. Zhou, F.-I. Li, B. Bai, H. Chen, J. Liu, Z. Xu, and H. Zheng, *Phys. Rev. A* **95**, 053809 (2017).
- [39] G. S. Agarwal and K. Tara, *Phys. Rev. A* **46**, 485 (1992).
- [40] K. Y. Spasibko, D. A. Kopylov, V. L. Krutyanskiy, T. V. Murzina, G. Leuchs, and M. V. Chekhova, *Phys. Rev. Lett.* **119**, 223603 (2017).
- [41] G. S. Agarwal, *Phys. Rev. A* **1**, 1445 (1970).
- [42] A. Jechow, M. Seefeldt, H. Kurzke, A. Heuer, and R. Menzel, *Nat. Photonics* **7**, 973 (2013).